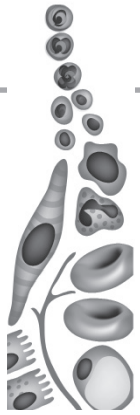

Characterization of the cells in repair tissue following autologous chondrocyte implantation in mankind: a novel report of two cases

Aim: Autologous chondrocyte implantation (ACI) is used worldwide for the treatment of cartilage defects. This study has aimed to assess for the first time the cells that are contained within human ACI repair tissues several years post-treatment. We have compared the phenotypic properties of cells from within the ACI repair with adjacent chondrocytes and subchondral bone-derived mesenchymal stromal/stem cells (MSCs). **Materials & methods:** Two patients undergoing arthroplasty of their ACI-treated joint were investigated. Tissue and cells were isolated from the repair site, adjacent macroscopically normal cartilage and MSCs from the subchondral bone were characterized for their growth kinetics, morphology, immunoprofile and differentiation capacity. **Results:** ACI repair tissue appeared fibrocartilaginous, and ACI repair cells were heterogeneous in morphology and size when freshly isolated, becoming more homogeneous, resembling chondrocytes from adjacent cartilage, after culture expansion. The same weight of ACI repair tissue resulted in less cells than macroscopically normal cartilage. During expansion, ACI repair cells proliferated faster than MSCs but slower than chondrocytes. ACI repair cell immunoprofiles resembled chondrocytes, but their differentiation capacity matched MSCs. **Conclusion:** This novel report demonstrates that human ACI repair cell phenotypes resemble both chondrocytes and MSCs but at different stages of their isolation and expansion *in vitro*.

KEYWORDS: autologous chondrocyte implantation ▪ differentiation potential ▪ growth kinetics ▪ histochemical analysis ▪ immunoprofile ▪ morphology ▪ phenotype ▪ repair cell characterization

Karina T Wright*[1,2], Claire Mennan[1,2], Hannah Fox[3], James B Richardson[1,2], Robin Banerjee[1] & Sally Roberts[1,2]

[1]Robert Jones & Agnes Hunt Orthopaedic Hospital, Oswestry, Shropshire, SY10 7AG, UK
[2]Institute for Science & Technology in Medicine, Keele University, Keele, Staffordshire, ST5 5BG, UK
[3]Department of Pathology, Cambridge University, Tennis Court Road, Cambridge, Cambridgeshire, CB2 1QP, UK
**Author for correspondence: Tel.: +44 169 140 4699 karina.wright@rjah.nhs.uk*

There is a huge interest worldwide in the development of tissue engineering and cell-based therapies for the treatment of cartilage defects. Autologous chondrocyte implantation (ACI) is a procedure that has been used for more than 20 years for the treatment of cartilage injury and osteoarthritis [1–3]. Our center has provided cells for over 400 ACI procedures since its inception, of which 81% were a success, as indicated by a postoperative increase in the Lysholm score [4]. What happens to the culture-expanded chondrocytes after implantation and the contribution that they make to the repair tissue compared with cells from surrounding tissues is still largely unknown [5–7]. Few preclinical studies have labeled and tracked transplanted chondrocytes in ACI models. Those that have show that varying proportions of the cells injected form the cellular component of the tissue at the site of ACI. In these studies transplanted cells have been shown to contribute in part to the formation and integration of repair tissues. However, numerous unlabeled cells also form a major constituent, which suggests that cells of unknown origin migrate to ACI-treated lesions and combine with transplanted cells as part of the healing process [6,7].

The purpose of this study is to describe for the first time the phenotype of those cells that are contained within the tissue at the site of ACI in humans several years after treatment. Characterization of the cells that are present at the site of ACI and, hence, the ones that are likely to produce and remodel the repair tissue, is critical to our understanding of the biological process in ACI. In previous studies we have only been able to assess the quality of ACI repair tissues in the clinic via MRI and histological analyses of small regions (<2-mm diameter cores) [8–11]. We have obtained two rare samples that have provided us with the opportunity to isolate and examine the behavior and phenotypic properties of ACI repair cells in culture, in comparison with both chondrocytes in the adjacent cartilage and MSCs from the subchondral bone. Observing ACI repair cells in culture will help to provide novel information on the cellular component of ACI repair tissues, which we can then compare with histological analyses and clinical outcome. In addition, by analyzing the properties of ACI repair cells in contrast to the phenotypes of cells isolated from neighboring tissues (e.g., cartilage and bone), we may begin to elucidate the ACI repair cell origin. Herein we describe the analysis

Regenerative Medicine

of repair tissues and cells from two former ACI patients that have returned to our clinic for arthroplasty of their ACI-treated joints several years post-ACI.

Materials & methods

Patient information

Following local research ethical committee approval and with informed consent, tissues obtained from two patients undergoing joint replacement surgery were included in this study (one knee [patient 1] and one hip [patient 2]). Both were males and the patients were aged 49 and 44 years at the time of arthroplasty, which was ~11 and ~5 years, respectively, after their previous ACI treatment (Table 1).

Histological analysis

For histological examination decalcified wax-embedded tissue sections from the region bridging macroscopically normal cartilage (MNC) and ACI repair tissues (with subchondral bone) from patients 1 and 2 were examined using hematoxylin and eosin (H&E) and toluidine blue (British Drug Houses [BDH], UK) stains, as described previously [12]. For H&E histological examination, sections were flooded with Mayer's hemalum (VWR International Ltd, UK) for 1 min, drained and washed in tap water for 5 min. Slides were then flooded with 1% eosin aqueous solution (BDH; in distilled water) for 30 s, briefly washed in tap water and dehydrated through a series of isopropanol (Genta Medical, UK) concentrations in distilled water and then xylene, for 5 min each. Following dehydration, the tissue sections were mounted under glass coverslips (Cell Path Ltd, UK) with Pertex mounting medium (Histolab Products AB, Sweden) and allowed to air dry. The glycosaminoglycan (GAG) content was assessed by metachromasia by flooding sections with 1% aqueous toluidine blue (BDH) solution for 30 s and rinsed in tap water. Slides were left to air dry before mounting under glass coverslips with Pertex mounting medium.

For collagen type II immunolocalization, dewaxed and rehydrated sections were pretreated with 0.1% (w/v) hyaluronidase and 0.2% (w/v) trypsin (Sigma-Aldrich, UK) for 1 h at 37°C. Sections were then washed in phosphate-buffered saline (PBS) and incubated for 2 h at room temperature in a humidified chamber with 10 µg/ml of primary mouse monoclonal collagen type II antibody (clone CIIC1, Developmental Studies Hybridoma Bank, University of Iowa, IA, USA) in PBS. Parallel sections were incubated with a nonspecific, isotype-matched antibody (IgG1; Dako, Denmark) instead of the primary antibody at the same concentration, as a negative control. After incubation with the primary antibodies, all sections were washed in PBS before incubation for 1 h with a secondary biotinylated antibody at 50 µg/ml (VECTASTAIN® ABC system, Vector Laboratories Ltd, UK) according to the manufacturer's protocol. To eliminate endogenous peroxidase activity sections were blocked with 0.3% (v/v) hydrogen peroxide in methanol (BDH) for 30 min. Collagen type II immunopositivity was finally visualized by testing for bound peroxidase, which is detected by incubation with a substrate of diaminobenzidine tetrahydrochloride, activated by hydrogen peroxide. The sections were then dehydrated before mounting under glass coverslips with Pertex mounting medium as described previously.

Chondrocyte & ACI repair cell isolation & culture

Approximately 300 mg of MNC and ACI repair tissues were harvested from the medial femoral condyle of patient 1 and the femoral head of patient 2. Cells were isolated and cultured as described previously for chondrocytes [13]. MNC and ACI repair tissues were dissected into approximately 2-mm^3 pieces and placed into 25-cm^2 tissue culture flasks (Falcon™ 250-ml Polystyrene Tissue Culture Flask, BD Biosciences, UK). The weight of each tissue type was recorded and cells released by enzymic digestion. DMEM/F12 (Life Technologies, UK) containing 0.8 mg/ml type XI collagenase (Sigma-Aldrich) was added to each of the flasks which were then incubated at 5% (v/v) CO_2 for 20 h at 37°C.

Following this incubation, each tissue digest was passed through a 70-µm cell strainer (BD Biosciences); cells were recovered by centrifugation at 750 × *g* for 10 min to form a cell pellet.

Table 1. Patient information: demographics and autologous chondrocyte implantation treatment received.

Patient	Time since ACI, months (years)	Site of ACI	Size of defect	Cells received	Patch received
1	135 (11.25)	Medial femoral condyle	25 × 15 mm	Knee chondrocytes	Periosteum
2	59 (4.9)	Lateral aspect of femoral head	12-mm diameter	Hip chondrocytes	Chondro-Gide®

ACI: Autologous chondrocyte implantation.

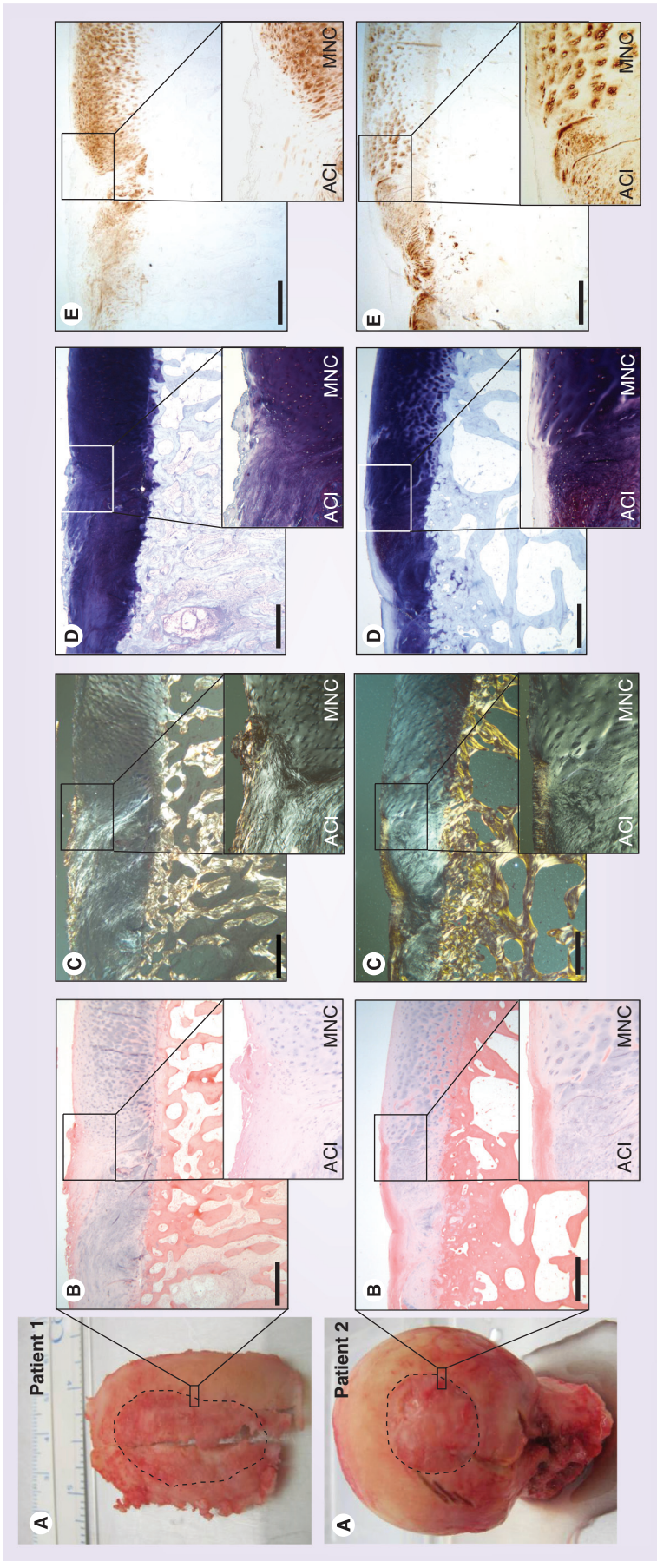

Figure 1. Histology of the autologous chondrocyte implantation: adjacent macroscopically normal cartilage interface. (A) Dotted line shows the ACI-treated areas. Samples received following arthroplasty are shown, demonstrating ACI repair regions at the center of the medial condyle (patient 1, top) and femoral head (patient 2, bottom). Regions dissected for histology are indicated (boxed). **(B)** Hematoxylin and eosin-stained sections showing a disorganized cell distribution in ACI repair tissues (left) compared with typical hyaline cartilage cell organization (right). **(C)** Polarized light illumination showing fibrocartilage (bright scatter) in ACI repair tissues (left), particularly evident at ACI–MNC interfaces (boxed). **(D)** Toluidine blue localization of glycosaminoglycans (GAGs) demonstrates that there are fewer GAGs present in ACI repair regions (left) compared with MNC (right). A dramatic reduction in GAG staining intensity is seen in the surface zone of ACI repair tissues. **(E)** Collagen type II immunolocalization demonstrates that ACI repair region matrices (left) contain less collagen type II compared with MNC (right). All scale bars = 1 mm.
ACI: Autologous chondrocyte implantation; MNC: Macroscopically normal cartilage.

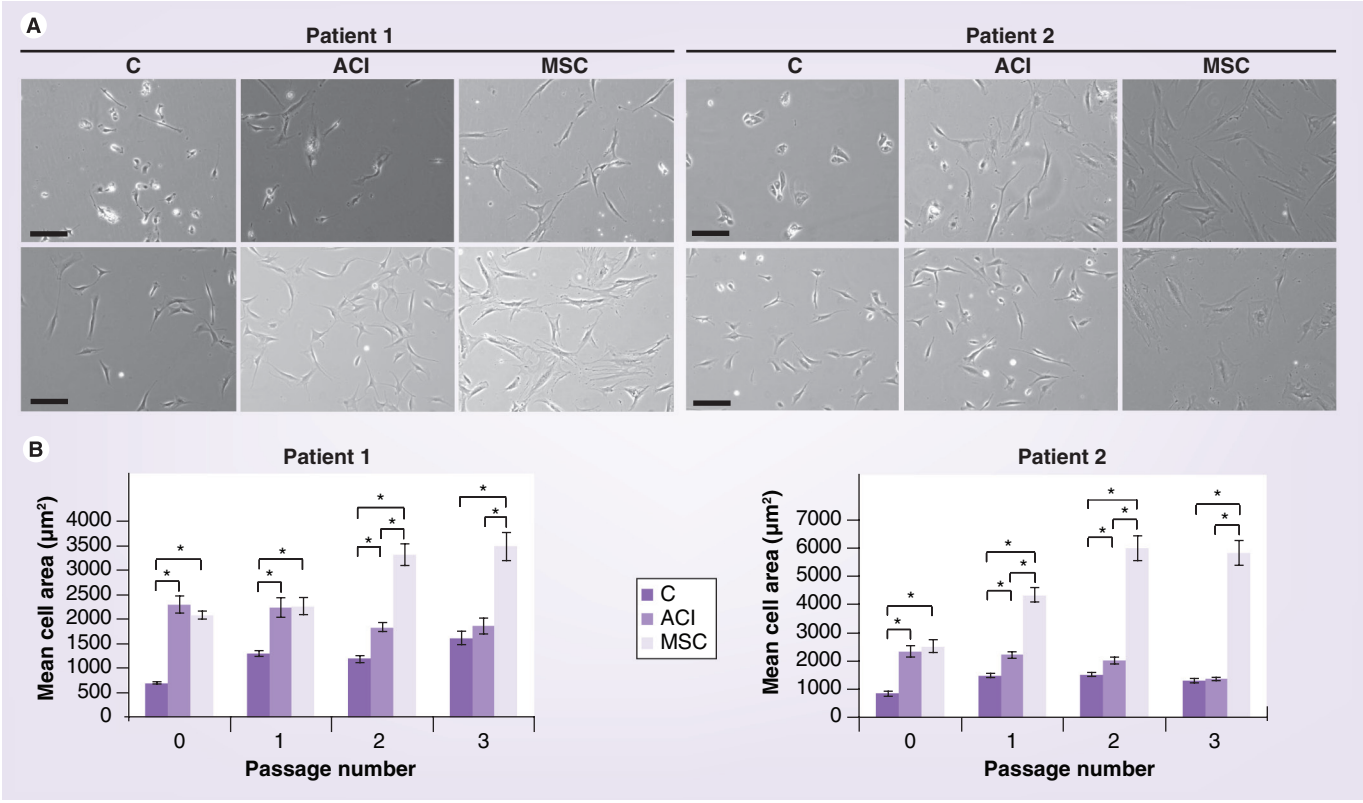

Figure 2. Cell characterization: morphology. (A) Freshly isolated cells are shown (top panels) compared with cells at passage 3 (bottom panels). Cs and MSCs isolated from both patients have a uniform fibroblast-like morphology that increases in size (area coverage) with subculture. Freshly isolated ACI repair cells show a heterogeneous morphology that becomes homogeneous at passage 3. All scale bars = 200 µm. **(B)** Cs and MSCs increase in size from passages 0–3. Cs are significantly smaller than MSCs at every passage quantified. At initial seeding ACI repair cells are significantly larger than Cs, but similar in size to MSCs. At passage 3 ACI repair cells are significantly smaller than MSCs, but similar in size to Cs. Data are demonstrated as mean ± standard error of the mean. Differences were calculated using the Kruskal–Wallis analysis of variance with the Bonferroni *post hoc* test.
*$p < 0.001$.
ACI: Autologous chondrocyte implantation; C: Chondrocyte; MSC: Mesenchymal stromal cell.

Cells were plated out in DMEM/F12, supplemented with 10% fetal bovine serum (FBS; Life Technologies), 50 µg/ml ascorbic acid (Sigma-Aldrich) and 1% (v/v) penicillin and streptomycin (P/S; Life Technologies) at a seeding density of 5×10^5 cells/cm^2. After 5 days, nonadherent cells were removed and the adherent cell population was cultured as a monolayer in DMEM/F12 10% FBS medium supplemented with ascorbic acid and P/S. Cells were routinely passaged at 70% confluence by trypsinization (0.05% v/v Trypsin–EDTA) and reseeded at 5×10^3 cells/cm^2.

Human bone MSC isolation & culture

The underlying bone from the medial femoral condyle of patient 1 and the femoral head of patient 2 was perfused with DMEM/F12 (Life Technologies) supplemented with 10% FBS and P/S. Mononuclear cells isolated and MSCs were cultured as described previously [14]. Mononuclear cells were isolated by density gradient centrifugation (Lymphoprep™, Fresenius Kabi Norge AS, Norway) were plated out in DMEM/F12, supplemented with 20% FBS and P/S at a seeding density of 20×10^6 cells per 25 cm^2 tissue culture flask. After 24 h, nonadherent cells were removed and the adherent cell population was cultured in monolayer in DMEM/F12 10% FBS medium supplemented with P/S. Cells were routinely passaged at 70% confluence by trypsinization (0.05% v/v Trypsin–EDTA) and reseeded at 5×10^3 cells/cm^2. Viability was assessed at each passage by trypan blue exclusion (Sigma-Aldrich).

Microscopy, image capture & analysis

Histological sections were viewed using bright light and polarized light microscopy (Leitz Diaplan, Germany) and digitized images were captured with a digital camera (DS-Fi1, Nikon, UK). Cultures were viewed using phase contrast microscopy (Nikon Eclipse TS100) and

digitized images were captured with a digital camera (C4742-95, Hamamatsu, NJ, USA). The mean cell area was determined from passage 0–3 for the three cell populations using IPLab software (Version 3.6, Biovision Technologies, PA, USA). For each cell type, results from at least five separate images per culture were combined.

Growth kinetics

Culture doubling time (DT) was calculated for each cell population (from passage 0–3) using the following formula: DT = $(t_2\text{-}t_1) \times \ln(2)/\ln(n2/n1)$, where t_1 = the time of cell seeding, t_2 = the time of cell harvest and n = the matching cell numbers at these time points.

Immunoprofiling

Immunoprofiling via flow cytometry was used to assess culture-expanded cells (at passage 2) using a FACScan™ flow cytometer (BD Biosciences). A profile typical of MSCs was targeted [15]. In brief, cells were blocked for 1 h in a buffer of 10% normal human immunoglobulin (Grifols, UK). Cells were then incubated with mouse antihuman monoclonal primary antibodies against CD14, CD19, CD31, CD34, CD45, CD73, CD90, CD105 and HLA-DR (all phycoerythrin-conjugated; Immunotools, Friesoythe, Germany) for 30 min. Matched cell populations were also exposed to isotype-matched IgG negative control antibodies (Sigma-Aldrich). Immunoprofiles were produced using CellQuest™ software (BD Biosciences).

Multipotency assays

Established protocols [16–18] were used to assay the differentiation potential of cells at passage 2 for adipogenic, osteoblastic and chondrogenic lineages. In brief, for 21 days, cell cultures were exposed to appropriate conditions for:

- Adipogenic differentiation via monolayer culture in DMEM/F12 10% fetal calf serum, 1% insulin transferrin selenium-X (Life Technologies), dexamethasone, 3-isobutyl-1-methylxanthine and indomethacin (Sigma-Aldrich);
- Osteoblastic differentiation via monolayer culture in DMEM/F12 10% fetal calf serum, ascorbate 2-phosphate, dexamethasone and β-glycerophosphate (Sigma-Aldrich);
- Chondrogenic differentiation via micromass pellet culture in DMEM/F12, 1% insulin transferrin selenium-X, ascorbate 2-phosphate (Sigma-Aldrich), dexamethasone (Sigma-Aldrich) and TGF-β1 (PeproTech Ltd, UK).

At the 21-day time point, adipogenic differentiation potential was examined via Oil Red O (Sigma-Aldrich) visualization of lipid formation, alkaline phosphatase activity was used to assess osteoblast differentiation, and for chondrogenic differentiation, toluidine blue staining was used to detect the presence of GAGs in micromass pellets.

Statistical analysis

The Kruskal–Wallis nonparametric analysis of variance and *post hoc* Bonferroni pairwise comparison tests were used to assess significant differences between the size (area coverage) of each cell type isolated from the same joint, for example, chondrocytes, ACI repair cells and MSCs between passages 0 and 3.

Results

Histological analysis

Tissue sections from the region bridging MNCs and ACI repair tissues (FIGURE 1A) were examined via H&E staining (FIGURE 1B), which demonstrated a disorganized cellular distribution throughout ACI repair tissues in both patients compared

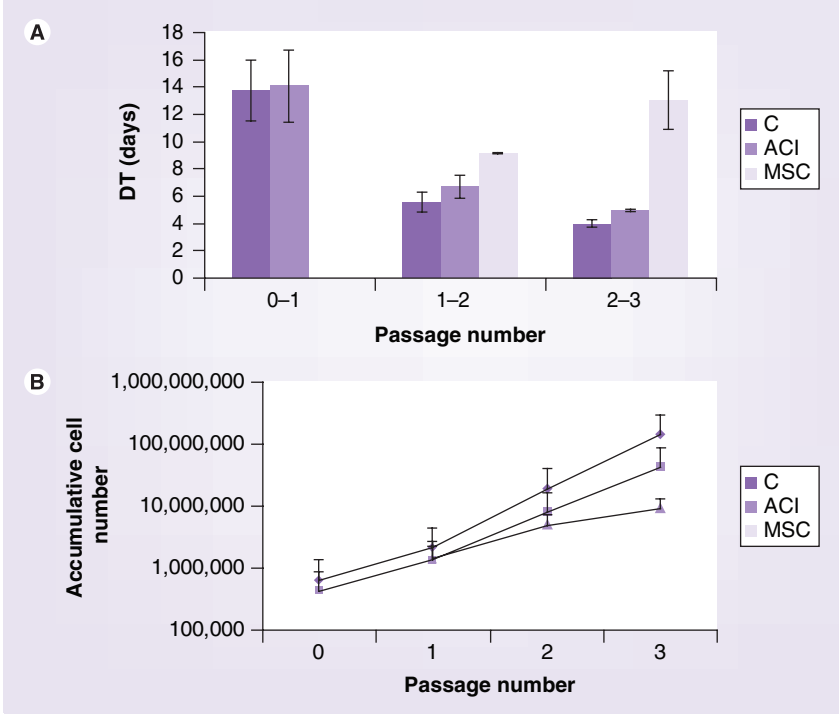

Figure 3. Cell characterization: growth kinetics. (A) The DTs of Cs and ACI repair cells decrease similarly through passages 0–3. By contrast, MSC DTs increase between passages 1–3. **(B)** After harvest at passage 3, C cultures produced 1.4×10^8 cells, ACI repair cultures 4.3×10^7 cells and MSC cultures 9.0×10^6 cells. Data are demonstrated as mean ± standard error of the mean from pooled patient data.
ACI: Autologous chondrocyte implantation; C: Chondrocyte; DT: Doubling time; MSC: Mesenchymal stromal cell.

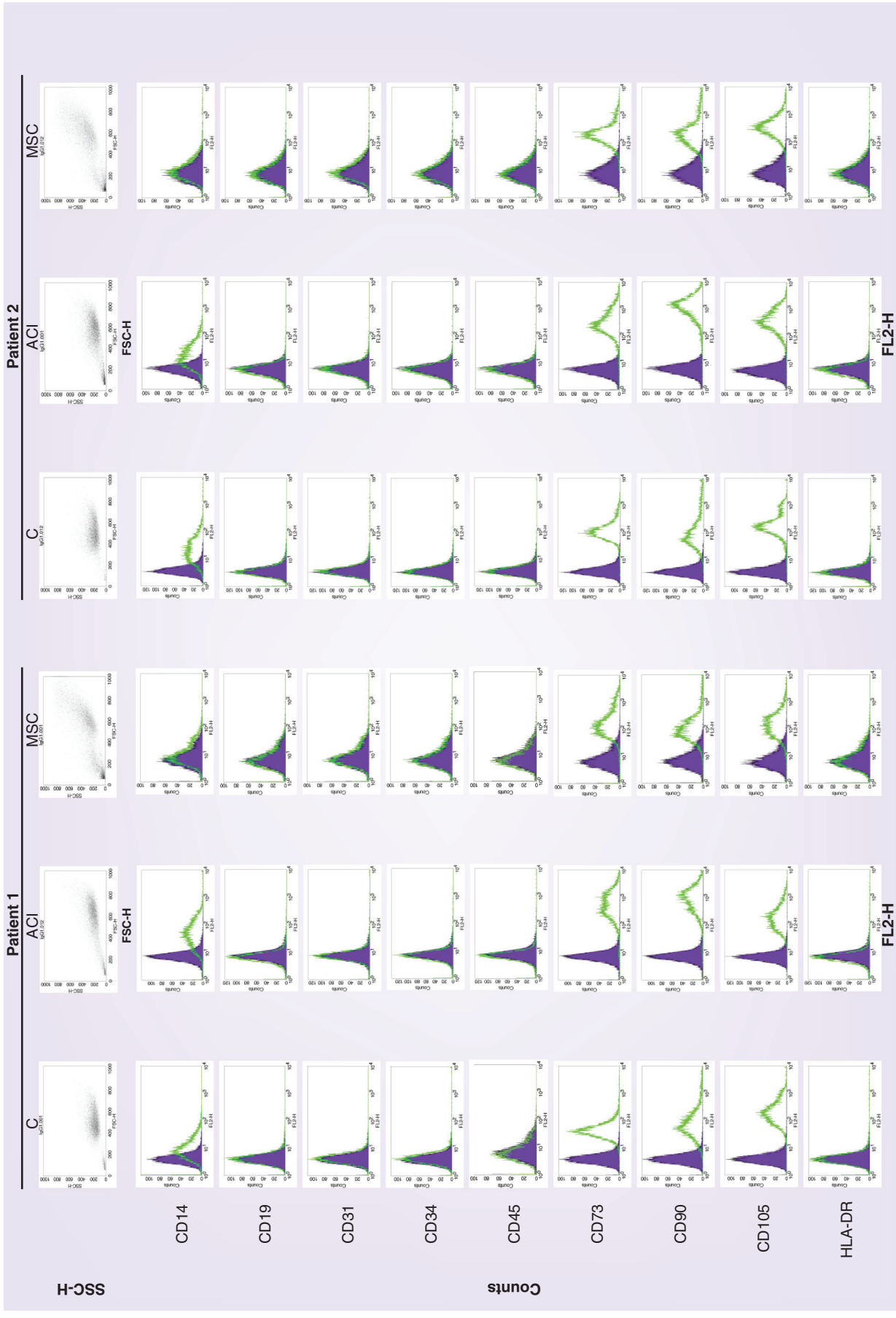

Figure 4. Phenotypic characterization: immunoprofile and differentiation capacity (passage 2 cells). Flow cytometry analysis for CD immunolabeling of Cs, ACI repair cells and MSCs. All cultures tested are CD19$^-$, CD31$^-$, CD34$^-$, CD45$^-$, CD73$^+$, CD90$^+$, CD105$^+$ and HLA-DR$^-$ at passage 2. Cs and ACI repair cells are also immunopositive for CD14 to varying degrees (patient 1: Cs ~50% and ACI ~90%; patient 2: Cs ~90% and ACI ~50%), whereas MSCs are CD14$^-$. The green-lined histogram denotes immunopositivity (fluorescence intensity) for each indicated marker, while the purple histogram denotes immunolabeling with an isotype-matched control antibody. See color figure at www.futuremedicine.com/doi/pdf/10.2217/rme.13.67.
ACI: Autologous chondrocyte implantation; C: Chondrocyte; MSC: Mesenchymal stromal cell.

with neighboring MNCs. There appeared to be good integration between the repair cartilage and the neighboring MNCs and the underlying bone. The surface integrity and smoothness of ACI repair tissues differed between patients; in the knee (patient 1) the repair surface was rough, whereas the hip repair tissue (patient 2) was smooth but undulating compared with neighboring MNCs, which were smooth and flat in both patients.

Viewing the same section under polarized light (FIGURE 1C) revealed illuminated areas of scattered light indicative of fibrocartilage throughout the repair region and in particular at the border with MNCs. Toluidine blue staining (FIGURE 1D) indicated that the GAG content of ACI repair tissues was lower than that of neighboring MNCs, particularly in the surface zone. For both patients collagen type II staining (FIGURE 1E) was similarly weaker in the surface zone of ACI repair tissues.

Morphological analyses

For both patients freshly isolated chondrocytes and MSCs had a uniform fibroblast-like morphology with their size (surface area coverage) increasing after expansion. MSCs appeared consistently larger at each passage compared with chondrocytes. In addition, for MSC cultures numerous intracellular stress fibers were clearly visible at passage 3. By contrast, the morphologies of freshly isolated ACI repair cells were more heterogeneous. ACI repair cells possessed a combination of early- and later-passage chondrocyte and MSC-like morphologies after initial seeding but became homogeneous after subculture. There were no obvious or significant differences between ACI and chondrocyte cultures (FIGURE 2A & 2B).

Growth kinetics

Chondrocytes and ACI repair cells proliferated at similar rates for both patients (from passages 0 to 3), with DTs of 2 weeks between passages 0–1, decreasing to 4–6 days between passages 1–2 and 2–3. By contrast, the DT of MSCs was markedly higher at 8–14 days between passages 1–2 and 2–3 (FIGURE 3A). At passage 3 chondrocyte cultures produced harvests of 1.4×10^8, ACI repair cells 4.3×10^7 and MSCs 9.0×10^6 (FIGURE 3B). Viability for all cells was >98% at each passage.

Immunoprofiles

MSCs from both patients were $CD14^-$, $CD19^-$, $CD31^-$, $CD34^-$, $CD45^-$, HLA-DR^-, $CD73^+$, $CD90^+$ and $CD105^+$; this matches previously published MSC immunoprofiles [15].

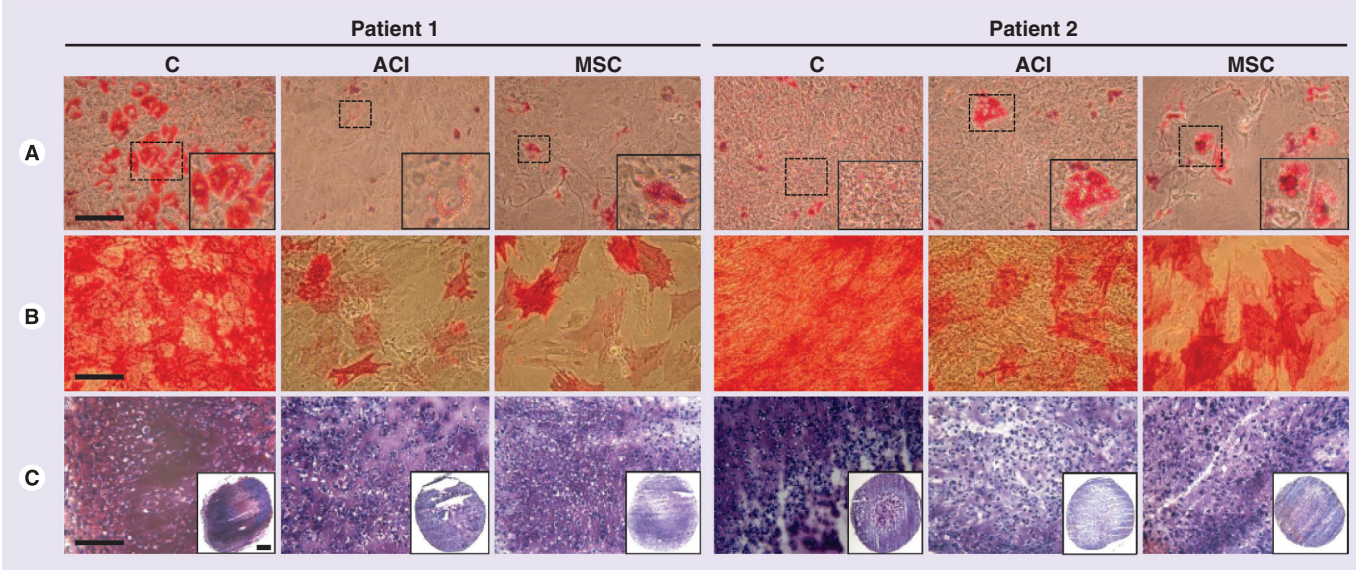

Figure 5. Phenotypic characterization: differentiation capacity (passage 2 cells). (A) The presence of lipid vesicles is increased in chondrocytes treated with adipogenic stimuli (but a different type of staining pattern between patients can be observed, as revealed with Oil Red O) compared with ACI repair cells or MSCs (which had similar localized unilocular lipid staining in patches). Dashed boxes indicate regions that have been expanded in the inserts (included in the bottom right corner) to highlight small lipid droplets. **(B)** Alkaline phosphatase activity is markedly increased in chondrocyte cultures treated with osteogenic stimuli compared with ACI repair cells or MSCs. **(C)** Toluidine blue staining of chondrogenically induced pellet cultures shows more intense staining in chondrocyte pellets compared with ACI repair cells or MSC pellets. Scale bars = 100 µm; inset scale bar = 200 µm. See color figure at www.futuremedicine.com/doi/pdf/10.2217/rme.13.67.
ACI: Autologous chondrocyte implantation; C: Chondrocyte; MSC: Mesenchymal stromal cell.

Chondrocytes and ACI repair cells from both patients had MSC-like immunoprofiles apart from some positivity for CD14; for patient 1 CD14 was detected on approximately 90% of chondrocytes and approximately 50% of ACI repair cells, whereas for patient 2 the reverse pattern of positivity was observed between chondrocytes (~50% immunopositive) and ACI (~90% immunopositive; Figure 4).

Differentiation potential

Chondrocytes, ACI repair cells and MSCs from both patients differentiated along all three mesenchymal cell lineages tested but to varying degrees, as delineated by lipid accumulation, alkaline phosphatase activity and toluidine blue GAG staining. Chondrocytes from patient 1 produced a large frequency of clustered globular lipids, whereas chondrocytes from patient 2 showed more diffuse staining of smaller lipids throughout. ACI and MSC staining for lipid accumulation was similar in pattern for both patients, hence, a few unilocular lipid clusters (which may be indicative of committed adipocytes) were seen in both (Figure 5A). Chondrocytes from both patients showed intense uniform staining for alkaline phosphatase activity, whereas ACI repair cells and MSCs demonstrated a more heterogeneous pattern of staining (Figure 5B). All pellet cultures showed the presence of some GAGs via toluidine blue staining. Chondrocyte fractions showed the most intense toluidine blue staining, ACI repair cell and MSC pellets showed weaker GAG staining for both patients (Figure 5C).

Discussion

These samples have provided a unique opportunity to study both the histology of the complete area of ACI repair tissue compared with neighboring MNC as well as examining the phenotype of ACI repair cells compared with chondrocytes from adjacent cartilage and MSCs from the underlying subchondral bone, several years post-ACI. For these analyses, tissues and cells were harvested from two former ACI patients at the time of arthroplasty. It is debatable whether the patients included in this study and, hence, the tissues and cells examined here, should be considered as ACI successes or failures. These individuals were 38 and 39 years of age at the time that they received ACI and although their treated joints ultimately failed, ACI prolonged the life of their natural joints for 11 and 5 years, respectively. For patients of such a young age this may have important implications for later life as joint replacement is accompanied by some loss of function that restricts activities [19]. In addition, joint replacements will probably not last for the full life of younger patients. Hence, the initial surgery may need revision, which is a more complicated and expensive operation with lower success rates than primary arthroplasty [20]. As such, ACI therapy that increases the lifespan of these young patients' joints may understandably be considered a successful intervention even though their treated joints eventually failed.

Histologically, we have shown that ACI repair tissues resembled those previously described [8–10]; cells were numerous but disorganized and matrices appeared predominantly fibrocartilaginous. Repair tissues were well integrated with adjacent MNC and subchondral bone. The surface of repair tissue for patient 1 was rough compared with that of patient 2, perhaps because patient 1 received a periosteal graft, which may exhibit hypertrophy, compared with the collagen membrane that was used for patient 2 [21]. There were no obvious histological signs that may have explained joint failure in these patients. However, there is limited evidence that histology is a reliable indicator of clinical outcome for ACI patients [22]. In this study we have some preliminary data for ACI repair cell characterization, which may represent a promising additional prognostic marker in future analyses. An understanding of the ACI repair cell phenotype will help to elucidate ACI repair tissue formation and remodeling processes. In addition, we may be able to use this data to begin to 'unpick' the origin of ACI repair cells and hence, to determine if ACI tissues contain any of those cells initially implanted at ACI stage II. In preclinical studies transplanted cells are known to persist in ACI repair zones for up to 14 weeks in large animal models [6]. Alternatively, the site of ACI repair may contain a completely different cell type (e.g., synovium, bone or bone marrow-derived MSCs) that has migrated and integrated into ACI zones from surrounding tissues [23–25].

It is likely that the anatomical location (i.e., knee versus hip) and the patch used at ACI (i.e., periosteum vs Chondro-Gide®, Geistlich Pharma, Switzerland) will have influenced the quality and extent of the repair tissue observed for patient 1 compared with patient 2. However, there were no discernible differences observed in the phenotypes of ACI repair cells isolated from patient 1 or patient 2. This suggests that the dissimilarities between these examples of ACI, that is, the type of joint treated and patch used, might not have contributed significantly to the tissue regeneration seen (or the cells involved) in these

ACI-treated joints. We have shown that freshly isolated cells from ACI repair tissues appeared to contain a mixture of chondrocyte and MSC morphologies, but that MSC-like cells disappear over time in culture. Our growth kinetics data support the theory that chondrocytes may have outgrown MSCs *in vitro*. In addition, the immunoprofiles of chondrocytes and ACI repair cells were similar after subculture; both demonstrated some CD14 positivity, a marker found on freshly isolated chondrocytes [26,27], compared with a complete absence of CD14 on MSCs at the same passage. It is unlikely that the source of $CD14^+$ cells that were cultured from ACI repair tissues represent MSCs that have migrated from surrounding tissues (e.g., MSCs from synovium and bone or bone marrow) as these MSCs do not express CD14 in an undifferentiated state [15,28]. It is conceivable that these cells instead either represent a proportion of the chondrocytes that were originally transplanted at ACI or that have migrated from adjacent cartilage. Alternatively, an MSC population may have homed to the injured region and differentiated *in vivo* towards a chondrogenic lineage [29,30].

Interestingly, our multipotency studies showed a marked contrast between passaged chondrocyte and ACI repair cell differentiation potential. Chondrocyte populations differentiated along adipogenic, osteogenic and chondrogenic lineages in a strongly positive and uniform manner as articular cartilage itself contains a multipotent progenitor cell population [31–35]. By contrast, ACI repair cells appeared heterogeneous and, on the whole, differentiated along each mesenchymal lineage tested to a lesser extent, akin to MSCs isolated from the same joint. However, we acknowledge that culture expansion may change the characteristics of ACI repair cells. It is therefore difficult to ascertain exactly how the immunoprofile and differentiation potential of culture-expanded ACI repair cells relate to their *in vivo* characteristics. Nonetheless, this study demonstrates that, although cultured ACI repair cells possess many phenotypic characeristics of chondrocytes (e.g., similar morphologies, growth kinetics and immunoprofiles), they do not possess the ability to differentiate, importantly in this setting, into chondrocytes with physiologically relevant properties. For example, ACI repair cells do not appear to synthesize GAG-rich matrices to the same extent as chondrocytes when chondrogenically induced *in vitro*. This finding coincides with our *in vivo* histological evidence, which clearly shows that ACI repair tissues possess a lower GAG content in comparison with neighboring MNC.

A limitation of this study is that it is based on only two human samples, making the findings difficult to interpret. We hope to expand and corroborate the findings of these pilot experiments by increasing the sample size of donors and expanding the molecules and markers to be investigated in longer-term studies. For example, immunohistochemical analyses to determine the presence of type X collagen as a marker of hypertrophy in repair tissues, and gene expression studies of isolated repair cells for osteogenic- and chondrogenic-associated molecules using quantitative real-time PCR would provide valuable additional data. Nonetheless, this pilot study has provided a rare opportunity to carry out studies that are normally only possible in animals, but even then at much shorter time points. The information obtained is therefore completely novel and likely to be more relevant to the human patient than results from animal studies.

Conclusion & future perspective

This study presents the first data on human ACI repair cell phenotypes in culture, several years after ACI treatment. Cells isolated from ACI repair tissue appeared to contain a mixture of chondrocyte and MSC morphologies at initial seeding, but became more like chondrocytes with regard to morphology, proliferation and immunoprofile at later passage. However, the differentiation potential of expanded ACI repair cells was reduced for each mesenchymal lineage tested compared with chondrocytes and notably so for chondrogenic potential, which is considerably relevant in this setting. These findings indicate that ACI repair cells are composed of a mixture of cells with features resembling both chondrocyte and MSC phenotypes. This suggests that ACI tissues contain both chondrocytes (either originally implanted or integrated from surrounding cartilage *in vivo*) and also MSCs that have infiltrated the treated region from synovium or subchondral bone. A better understanding of the source of cells that contribute to the repair tissue in ACI, especially when associated with the best clinical outcome, will provide valuable information to help improve the ACI technique in the clinic. For example, we may be able to select the most effective cells prior to implantation or to augment the migration of desirable endogenous cells from the nearby tissues. In this way we can make step changes and improvements in current cell therapy treatments of chondral defects.

Financial & competing interests disclosure

The authors are grateful to Arthritis Research UK for supporting this work (grant no. 19429 and 18480), to the Wellcome Trust for supporting H Fox and to The John Charnley Laboratory, RJAH Orthopaedic Hospital (UK), for the expansion and preparation of harvested chondrocytes used in the autologous chondrocyte implantation procedures. The authors have no other relevant affiliations or financial involvement with any organization or entity with a financial interest in or financial conflict with the subject matter or materials discussed in the manuscript apart from those disclosed.

No writing assistance was utilized in the production of this manuscript.

Ethical conduct of research

The authors state that they have obtained appropriate institutional review board approval or have followed the principles outlined in the Declaration of Helsinki for all human or animal experimental investigations. In addition, for investigations involving human subjects, informed consent has been obtained from the participants involved.

Executive summary

Patient information

- We have analyzed tissues and cells isolated from regions of repair in two patients undergoing arthroplasty several years after cell therapy with autologous chondrocytes; these have been compared with tissues and cells derived from adjacent cartilage and bone.

Histological analysis

- Autologous chondrocyte implantation (ACI) repair tissues were densely populated with cells but the extracellular matrix was disorganized and contained little glycosaminoglycan or collagen type II in surface zones compared with adjacent, macroscopically normal cartilage.

Morphological analyses

- Cells which were isolated freshly from ACI repair tissues had a mixture of chondrocyte and mesenchymal stromal/stem cell-like morphologies.

Growth kinetics, immunoprofiles & differentiation potential

- Following culture expansion, cells isolated from ACI repair tissues resembled chondrocytes in terms of their growth and immunoprofile but their adipogenic, osteogenic and (importantly) chondrogenic differentiation capacity was markedly reduced in comparison with chondrocytes isolated from adjacent macroscopically normal cartilage.

References

Papers of special note have been highlighted as:
- ▪ of interest
- ▪▪ of considerable interest

1 Brittberg M, Lindhall A, Nilsson A, Ohlsson C, Isaksson, O, Peterson L. Treatment of deep cartilage defects in the knee with autologous chondrocyte transplantation. *N. Engl. J. Med.* 331, 889–895 (1994).

▪▪ **First description of autologous chondrocyte implantation in humans where cultured autologous articular chondrocytes can be used to repair deep cartilage defects of the knee.**

2 Richardson JB, Caterson, B, Evans EH, Ashton BA, Roberts S. Repair of human articular cartilage after implantation of autologous chondrocytes. *J. Bone Joint Surg. Br.* 81, 1064–1068 (1999).

3 Corpus KT, Bajaj S, Daley E *et al.* Long-term evaluation of autologous chondrocyte implantation: minimum 7-year follow-up. *Cartilage* 3, 342–350 (2012).

4 Bhosale AM, Kuiper JH, Johnson WE, Harrison, PE, Richardson JB. Midterm to long-term longitudinal outcome of autologous chondrocyte implantation in the knee joint. *Am. J. Sports Med.* 37, 131S–138S (2009).

5 Grande DA, Pitman MI, Peterson L, Menche D, Klein M. The repair of experimentally produced defects in rabbit articular cartilage by autologous chondrocyte transplantation. *J. Orthop. Res.* 7, 208–218 (1989).

6 Dell'Accio F, Vanlauwe J, Bellemans J, Neys J, De Bari C, Luyten FP. Expanded phenotypically stable chondrocytes persist in the repair tissue and contribute to cartilage matrix formation and structural integration in a goat model of autologous chondrocyte implantation. *J. Orth. Res.* 21, 123–131 (2003).

7 Miot S, Gianni-Barrera R, Pelttari K *et al.* *In vitro* and *in vivo* validation of human and goat chondrocyte labelling by green fluorescent protein lentivirus transduction. *Tiss. Eng. Part C Methods* 16, 11–21 (2010).

8 Roberts S, McCall IW, Darby AJ *et al.* Autologous chondrocyte implantation for cartilage repair: monitoring its success by magnetic resonance imaging and histology. *Arthritis Res. Ther.* 5, R60–R73 (2003).

9 Tins BJ, McCall IW, Takahashi T *et al.* Autologous chondrocyte implantation in knee joint: MR imaging and histologic features at 1-year follow-up. *Radiology.* 234, 501–508 (2005).

10 Sharma A, Wood LD, Richardson JB, Roberts S, Kuiper NJ. Glycosaminoglycan profiles of repair tissue formed following autologous chondrocyte implantation differ from control cartilage. *Arthritis Res. Ther.* 9, R79–R88 (2007).

11 Roberts S, Menage J, Sandell SJ, Evans EH, Richardson JB. Immunochemical study of collagen types I and II and procollagen IIA in human cartilage repair tissue following autologous chondrocyte implantation. *Knee* 16, 398–404 (2009).

12 Roberts S, Menage J. Microscopic methods for the analysis of engineered tissues. In: *Biopolmer Methods in Tissue Engineering.* Hollander AP, Hatton PV (Eds). Humana Press, NJ, USA 177–185 (2004).

13 Harrison PE, Ashton IK, Johnson WE, Turner SL, Richardson JB, Ashton BA. The *in vitro* growth of human chondrocytes. *Cell Tissue Bank.* 1, 255–260 (2001).

14 Wright KT, El Masri W, Osman A *et al.* Bone marrow stromal cells stimulate neurite outgrowth over neural proteoglycans (CSPG), myelin associated glycoprotein and Nogo-A. *Biochem. Biophys. Res. Comm.* 354, 559–566 (2007).

15 Dominici M, Le Blanc K, Mueller I *et al.* Minimal criteria for defining multipotent mesenchymal stromal cells. The International Society for Cellular Therapy Position Statement. *Cytotherapy* 8, 315–317 (2006).

- **The International Society for Cellular Therapy Position Statement for defining the minimum criteria for multipotent mesenchymal stromal cells.**

16 Jaiswal N, Haynesworth SE, Caplan AI, Bruder S. Osteogenic differentiation of purified culture-expanded human mesenchymal stem cells *in vitro*. *J. Cell. Biochem.* 64, 295–312 (1997).

17 Johnstone B, Hering TM, Caplan AI, Goldberg VM, Yoo JU. *In vitro* chondrogenesis of bone marrow-derived mesenchymal progenitor cells. *Exp. Cell Res.* 238, 265–272 (1998).

18 Pittenger MF, MacKay AM, Beck SC *et al.* Multilineage potential of adult human mesenchymal stem cells. *Science* 284, 143–147 (1999).

- **Provides existence of multipotent mesenchymal stem cells in bone marrow.**

19 Scott CE, Bugler KE, Clement ND, MacDonald D, Howie CR, Biant LC. Patient expectations of arthroplasty of the hip and knee. *J. Bone Joint Surg. Br.* 94, 974–981 (2012).

20 Labek G, Thaler M, Janda W, Agreiter M, Stockl B. Revision rates after joint replacement: cumulative results from worldwide joint register data sets. *J. Bone Joint Surg.* 93, 293–297 (2011).

21 Gooding CR, Bartlett W, Bentley G, Skinner JA, Carrington R, Flanagan A. A prospective, randomized study comparing two techniques of autologous chondrocyte implantation for osteochondral defects in the knee: periosteum covered versus type I/III collagen covered. *Knee* 13, 203–210 (2006).

22 Hanifi A, Richardson JB, Kuiper JH, Roberts S, Pleshko N. Clinical outcome of autologous chondrocyte implantation is correlated with infrared spectroscopic imaging-derived parameters. *Osteoarthritis Cartilage* 20, 988–996 (2012).

23 Shapiro F, Koide S, Glimcher MJ. Cell origin and differentiation in the repair of full-thickness defects of articular cartilage. *J. Bone Joint Surg.* 75, 532–553 (1993).

24 De Bari C, Dell'Accio F, Tyzanowski P, Luyten FP. Multipotent mesenchymal stem cells from adult human synovial membrane. *Arthritis Rheum.* 44, 1928–1942 (2001).

25 Kurth TB, Dell'Accio F, Crouch V, Augello A, Sharpe PT, De Bari C. Functional mesenchymal stem cell niches in adult mouse knee joint synovium *in vitro*. *Arthritis Rheum.* 63, 1289–1300 (2011).

26 Diaz-Romero J, Nesic D, Grogan SP, Heini P, Mainl-Varlet P. Immunophenotypic changes of human articular chondrocytes during monolayer culture reflect bona fide dedifferentiation rather than amplification of progenitor cells. *J. Cell. Physiol.* 214, 75–83 (2007).

27 Lee HJ, Choi BH, Min BH, Park SR. Changes in surface markers of human mesenchymal stem cells during the chondrogenic differentiation process *in vitro*. *Arthritis Rheum.* 60, 2325–2332 (2009).

28 Rosengren S, Boyle DL, Firestein GS. Acquisition, culture, and phenotyping of synovial fibroblasts. *Methods Mol. Med.* 135, 365–375 (2007).

29 Summers KL, O'Donnel JL, Hoy MS *et al.* Monocyte-macrophage antigen expression on chondrocytes. *J. Rheumatol.* 22, 1326–1334 (1995).

30 Steck E, Fischer J, Lorenz H, Gotterbarm T, Jung M, Richter W. Mesenchymal stem cell differentiation in an experimental cartilage defect: restriction of hypertrophy to bone-close neocartilage. *Stem Cells Dev.* 18, 969–978 (2009).

31 de la Fuente R, Abad JL, García-Castro J *et al.* Dedifferentiated adult articular chondrocytes: a population of human multipotent primitive cells. *Exp. Cell Res.* 297, 313–328 (2004).

32 Alsalameh S, Amin R, Gemba T, Lotz M. Identification of mesenchymal progenitor cells in normal and osteoarthritic human articular cartilage. *Arthritis Rheum.* 50, 1522–1532 (2004).

33 Dowthwaite GP, Bishop JC, Redman SN *et al.* The surface of articular cartilage contains a progenitor cell population. *J. Cell Sci.* 117, 889–897 (2004).

- **Provides evidence of chondroprogenitor stem cell populations in articular cartilage.**

34 Grogan SP, Miyaki S, Asahara H, D'Lima DD, Lotz MK. Mesenchymal progenitor cell markers in human articular cartilage: normal distribution and changes in osteoarthritis. *Arthritis Res. Ther.* 11, R85–97 (2009).

35 Koelling S, Kruegel J, Irmer M *et al.* Migratory chondrogenic progenitor cells from repair tissue during the later stages of human osteoarthritis. *Cell Stem Cell* 4, 324–325 (2009).